Large-amplitude compression waves in an adiabatic two-fluid model of a collision-free plasma

By K. W. MORTON

Courant Institute of Mathematical Sciences, New York

(Received 1 May 1962)

The development of large amplitude compression waves in a collision-free plasma is studied by considering the motion of a plane piston into a uniform stationary plasma containing a magnetic field parallel to the plane of the piston. The adiabatic two-fluid equations are solved by finite-difference methods and the form of the waves after a long time is compared with the possible steady-state solutions.

A generalized discontinuous solution of the steady-state equations is found for sufficiently high Mach numbers. At the highest Mach numbers this leads to a constant state at the piston; while at lower speeds a wave train results whose amplitude increases as the speed decreases. In each of these cases the numerical solutions of the time-dependent equations converge rapidly to the steady-state solutions. At still lower speeds, where the solitary-wave solution exists, the situation is less clear.

1. Introduction

Finite-amplitude hydromagnetic waves in a cold two-component plasma with no collisions have been the subject of considerable attention since Adlam & Allen (1958) described the transverse solitary wave. Davis, Lüst & Schlüter (1958) have found periodic waves and Gardner & Morikawa (1960) have studied the asymptotic time-dependent behaviour near an equilibrium state disturbed by the motion of a piston. These are all transverse one-dimensional waves, the magnetic field being perpendicular to the direction of propagation of the waves. More recently, Saffman (1961*a*, *b*) has studied longitudinal waves and those in which the initial magnetic field has an arbitrary orientation.

The simplest extension of the equations to embrace a warm plasma involves the introduction of an isotropic adiabatic pressure: this has been called the adiabatic two-fluid model by Gardner *et al.* (1958) who considered it as a possible first-order approximation to a collision-free shock theory. They showed that solitary waves and periodic steady-state solutions also exist for the transverse case and these have been studied in detail by Morawetz (1959), Baños & Vernon (1960) and Vernon (1960).

Our aim in this paper is to study the development of a large-amplitude compression wave travelling across a magnetic field by using numerical methods, and to relate the situations holding after long intervals of time with the known steady-state solutions. The specific problem on which attention has been focused is the

following: we have a half space of plasma at rest and with uniform density, bounded by a plane, perfectly conducting piston, and containing a constant magnetic field parallel to the plane of the piston. The piston is now accelerated into the plasma to a final velocity at which it is held hereafter. The problem is to find the ensuing motion of the plasma and the changes in the magnetic field. Initially we asked the particular question: does the wave always break as in conventional non-dissipative fluid dynamics? This corresponds in the cold-plasma case to the looping of the particle orbits and is known to occur at a Mach number of two. To enable the solutions to be continued beyond this point we have introduced a von Neumann–Richtmyer artificial viscosity.

The first result, suggested by the behaviour of the numerical solutions, is that 'for sufficiently strong shocks' there exists a generalized solution of the steady-state equations that is discontinuous in the fluid variables. This is described in § 3, which contains a complete account of the steady-state solutions. Briefly, there are always two constant states and the types of solution that exist depend on the compression ratio η between the states and the ratio β_0 of the fluid to magnetic pressure in the initial state. The (η, β_0)-plane is divided into three main regions: (i) for small η, the solitary wave and, except for very small β_0, all the associated periodic waves exist; (ii) the solitary wave ceases to exist when, at its peak, the flow speed exceeds the characteristic speed and then only some of the periodic waves exist; and (iii) when the characteristic speed exceeds the flow speed in the second constant state, the discontinuous solution appears. The two constant states have different entropies and only in case (iii) can they be joined by a solution.

The numerical solutions of the time-dependent equations show a very close relationship to the steady-state solutions: in case (iii) the convergence to the steady-state solution is very rapid; and in case (ii), although convergence is not so rapid, a very close identification can be made between the actual solution and one composed from the steady-state solutions. This solution consists of a discontinuous leading edge followed by a wave train, the first waves of which are the largest periodic solutions that exist in the particular case. In case (i) the leading edge appears to be no longer discontinuous and no such identification has been found possible.

Similar work has been described by Auer, Hurwitz & Kilb (1961, 1962). Their results are identical to ours when no breaking occurs, but they use a semi-physical model to treat the breaking and then obtain results which appear quite different.

2. The equations of motion

We consider an infinite piston lying in the (y, z)-plane and moving in the positive x-direction so that all quantities depend only on x and the time t. Then, with the magnetic field B confined to the z-direction, the only other electromagnetic quantities occurring in the equations are E and J, the y-components of the electric field and current.

In the present approximation we assume quasi-neutrality of charge and a total ion and electron pressure p that is isotropic in the (x, y)-plane† and satisfies a

† The velocity dispersion in the z-direction is unaffected.

perfect gas law with adiabatic exponent $\gamma = 2$. Then the motion of the electrons and ions is described by the moment equations (derivable from the collisionless Boltzmann equation) in terms of their total mass density ρ, their common velocity u in the x-direction, the pressure p, and the total internal energy density $\bar{e}$.

The full set of equations can be written in dimensionless form after the introduction of the following characteristic quantities:

$a_0 = B_0/(\mu\rho_0)^{\frac{1}{2}}$, the initial Alfvén speed;

$\beta_0 = p_0/(B_0^2/2\mu)$, the ratio of the initial fluid and magnetic pressures;

$x_0 = (-e_+e_-\mu\rho_0/m_+m_-)^{-\frac{1}{2}} = (\mu\kappa\omega_p^2)^{-\frac{1}{2}}$, the characteristic length.

This length may be regarded either as the ratio of the speed of light $(\mu\kappa)^{-\frac{1}{2}}$ to the plasma frequency ω_p or as the geometric mean of the gyromagnetic radii of the ions and electrons moving across the initial field with speed a_0. Here we have used rationalized M.K.S. units, μ is the magnetic permeability of free space, and m_+, m_- and e_+, e_- are the ion and electron masses and charges.

Finally, normalizing to an initial density and magnetic field of unity, we obtain the following equations.

Conservation of mass:	$\rho_t + (\rho u)_x = 0.$	(2.1)
Conservation of x-momentum:	$\rho(u_t + uu_x) + p_x = JB.$	(2.2)
Conservation of y-momentum:	$J_t + (uJ)_x = \rho(E - uB).$	(2.3)
Conservation of energy:	$\bar{e}_t + [u(\bar{e}+p)]_x = JE.$	(2.4)
Maxwell's equations:	$B_t + E_x = 0, \quad B_x + J = 0.$	(2.5,6)

It is convenient to introduce, instead of the current J, the difference velocity†

$$v = J/\rho, \tag{2.7}$$

in terms of which the internal energy becomes

$$\bar{e} = \tfrac{1}{2}\rho(u^2 + v^2) + p. \tag{2.8}$$

Equation (2.3) is then replaced by

$$v_t + uv_x = E - uB, \tag{2.9}$$

which combined with (2.1) and (2.5) can be integrated to yield

$$v_x = \rho - B. \tag{2.10}$$

The initial conditions (and those at $x = +\infty$, $t > 0$) are:

$$\rho = B = 1, \quad p = \tfrac{1}{2}\beta_0, \quad E = u = v = 0. \tag{2.11}$$

We assume the piston to be a perfect conductor: thus E equals uB just inside the plasma and, from (2.9), it follows that the derivative of v along the piston path is zero. The boundary conditions at the piston are then

$$u = u_P(t), \quad \text{prescribed}; \quad v = 0. \tag{2.12}$$

† The actual difference between the ion and electron velocities is

$$(-e_+e_-/m_+m_-)^{\frac{1}{2}}\,(m_+/e_+ - m_-/e_-)\,v.$$

It will be noticed that when $\beta_0 = 0$ these boundary conditions, together with equation (2.2), will not allow the piston to be accelerated. For $\beta_0 > 0$, a boundary layer will develop at the piston which will become increasingly severe as $\beta_0 \to 0$ and prevent us from computing the limiting case.

This set of equations is not purely hyperbolic: the conservation equations have the usual characteristics for non-dissipative fluid flow; but by taking the speed of light as infinite Maxwell's equations, in particular (2.6) and (2.10), are parabolic in character. In the limit of small field gradients, however, v is identically zero and we are led to the simple one-fluid theory arising from the assumption of perfect conductivity. The equations reduce to those of ordinary fluid dynamics with a total pressure $p + \frac{1}{2}B^2$ and we have the usual phenomena of steepening compression waves and broadening rarefaction waves.

Thus we would expect some initial steepening of waves generated by moving the piston into the plasma, until the diffusive effects of the parabolic field equations take over. These may be sufficient to prevent completely the breaking of weak waves but at Mach numbers around two, which in the cold-plasma case corresponds to the onset of orbit crossings, breaking will still occur. The nature of the discontinuity formed in this case is readily apparent from the equations. If ρ and B remain finite then so, by equation (2.10), will v_x. Thus there will be no jump in B or v but only in the fluid quantities ρ, u and p: and the jump conditions must be just the Rankine–Hugoniot relations in these variables.

3. Steady-state solutions of the equations

In this section we shall consider solutions of the equations of § 2 which are steady when viewed from a frame of reference moving with a constant velocity U, the 'shock' velocity. These have been studied quite extensively by previous authors, the most complete description being that of Vernon (1960)—see also Baños & Vernon (1960). However, the existence of discontinuous solutions seems to have been completely overlooked: although when the restriction to a completely cold plasma both in front of and behind the wave is made, this possibility no longer exists.

The solitary wave first described by Adlam & Allen (1958), and the periodic waves by Davis *et al.* (1958), as well as the discontinuous solution, are all involved in describing the steady state eventually attained in the piston problem. So we shall give a complete description of all the steady-state solutions. Our approach is essentially that of Morawetz (1959).

With the use of primes to denote quantities referred to the moving frame of reference, the conservation equations become on integration

$$\rho u' = -U, \tag{3.1}$$

$$-Uu' + p + \tfrac{1}{2}B^2 = U^2 + \tfrac{1}{2}\beta_0 + \tfrac{1}{2}, \tag{3.2}$$

and

$$-u'(\bar{e}' + p) + UB = U\beta_0 + \tfrac{1}{2}U^3 + U, \tag{3.3}$$

where the constants of integration have been determined from the initial state; in the last equation we have used the deduction from (2.5) that

$$E' = E + UB = \text{const.} = U.$$

Now we replace the density ρ by the specific volume $V = \rho^{-1}$ and substitute into (3.3) the expressions for u' obtained from (3.1), that for p from (3.2), and for $\bar{e}'$ from (2.8). The result is a quadratic for V in terms of B and v:

$$3U^2V^2 - 2V(2U^2 + 1 + \beta_0 - B^2) + (U^2 - v^2 - 2B + 2 + 2\beta_0) = 0. \tag{3.4}$$

The remaining equations (2.10) and (2.6) become

$$V\,dv/dx + BV - 1 = 0 \tag{3.5}$$

and

$$V\,dB/dx + v = 0. \tag{3.6}$$

Thus solutions are described by this pair of equations for B and v with V defined by one of the roots of (3.4). Constant states correspond to singular points of the differential equations, given by $v_i = 0$, $B_iV_i = 1$. If we substitute $1/B$ for V in (3.4) with $v = 0$, we find one root corresponding to the initial state $B_0 = V_0 = 1$, and the other, $B_1 = \eta = 1/V_1$, which we would like to identify with a final state and for which

$$U^2 = 2(1 + \beta_0)\,\eta/(3 - \eta). \tag{3.7}$$

As the conditions in the constant states are just those corresponding to the assumption of perfect conductivity, equations (3.1) to (3.3) reduce in this case to the Rankine–Hugoniot conditions for the single fluid with a total pressure $p + \frac{1}{2}B^2$ and energy $\bar{e} + \frac{1}{2}B^2V$. Hence equation (3.7) is the usual Prandtl shock relation

$$\mu^2 u_0'^2 + (1 - \mu^2)\,c_0^2 = u_0'\,u_1', \tag{3.8}$$

where $\mu^2 = \frac{1}{3}$ and $c_0^2 = 1 + \beta_0$. Clearly, when the compression ratio η is greater than unity, the shock velocity U is greater than the magneto-sonic speed $(1 + \beta_0)^{\frac{1}{2}}$.

The solutions themselves are most conveniently described in the (B, v)-plane: with these co-ordinates, equations (3.5) and (3.6) define a direction field on a two-sheeted surface, each sheet corresponding to a root of the quadratic (3.4) for V. The form of each solution is determined by its behaviour near the two singular points and the nature of the roots for V. We consider the singular points first.

The discriminant for the characteristic equation takes on the simple form $V^{-2}\,\partial(VB)/\partial B$ at the singular points, which on computing the derivative becomes

$$\Delta_i = (M_i^2 - 1 - \beta_i)/V_i(M_i^2 - \beta_i) \quad (i = 0, 1). \tag{3.9}$$

Here $M_i^2 = u_i'^2\rho_i/B_i^2 = V_i^3U^2$ is the square of the Alfvén Mach number, and $\beta_i = 2p_i/B_i^2$ is the ratio of the fluid to the magnetic pressure. At the initial state $M_0^2 = U^2 \geqslant 1 + \beta_0$ for $\eta \geqslant 1$, so that this singular point is always a saddle point in the cases we are interested in. It is also easily ascertained that it always lies on the sheet corresponding to the larger of the roots for V. At the second singular point M_1^2 is always less than $1 + \beta_1$, so that we have a centre if $M_1^2 > \beta_1$ and a saddle point if $M_1^2 < \beta_1$. This condition can be written in the form:

$$\text{saddle point if} \quad 3(\eta - 1)/\eta^2(3 - \eta) > 1/(1 + \beta_0), \tag{3.10}$$

from which it is apparent that it is satisfied only for sufficiently large η. It can also be shown that when this is so the singular point lies on the sheet of the smaller V root. Thus in the only case when solutions may issue from both singular points

they are on different sheets and may, in general, be joined only by a discontinuity in V.

The two sheets corresponding to the roots for V are joined on a closed convex curve on which the roots are equal. Inside the curve the roots become complex so that no physically admissible solution may cross into this region. If we write the equation for the curve in the form

$$\{B^2-3(1+\beta_0)(\eta-1)/(3-\eta)\}^2-12(1+\beta_0)B(B-\eta)/(3-\eta)+3U^2v^2=0, \quad (3.11)$$

we see that it always lies to the right of the second singular point ($B_1=\eta$, $v_1=0$), passing through it when (3.10) becomes an equality: as observed above it is at this point that the second singular point changes from one sheet to the other.

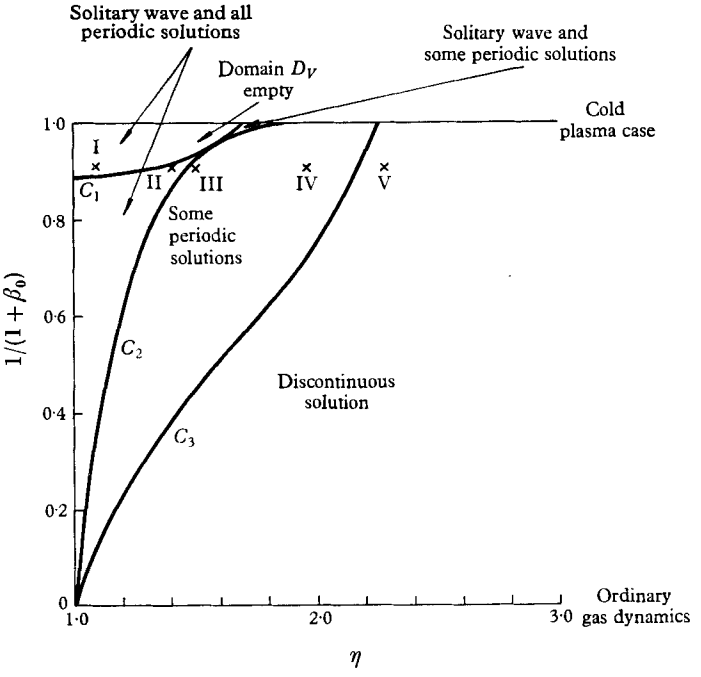

FIGURE 1. Domains of existence of the steady-state solutions and the positions of cases I to V.

We can now give a complete description of the three main types of steady-state solution. For any given value of β_0 ($0 \leqslant \beta_0 \leqslant \infty$) the situation depends on one other parameter describing the 'shock' strength: this could be either U or η, which are related by equation (3.7), but because of the convenience of its range of possible values ($1 \leqslant \eta \leqslant 3$) we shall use the latter. The values of these parameters for which each situation holds are shown in figure 1 and typical situations in the (B, v)-plane are shown in figure 2.

For sufficiently weak disturbances, i.e. η near unity, a solitary-wave solution exists and appears as a lobe in the (B, v)-plane about the centre at $B_1=\eta$, $v_1=0$; inside this is a complete set of periodic solutions of increasing entropy and decreasing amplitude as they circle nearer and nearer to the centre. This situation holds because either the domain D_V, containing the complex roots for V, is empty

or lies to the right of the solitary-wave lobe. D_V is empty in the region above and to the left of the curve C_1 in figure 1; on this curve it appears as a single point which for $\beta_0 > 0{\cdot}03704$ (or $\eta < 1{\cdot}6$) is outside the solitary wave, while otherwise it is inside. In the latter case, as η is increased D_V expands excluding more and more of the periodic solutions until it intersects the solitary-wave lobe; this region is shown as a small triangle bounded by curves C_1, C_2 and the line $\beta_0 = 0$ in figure 1.

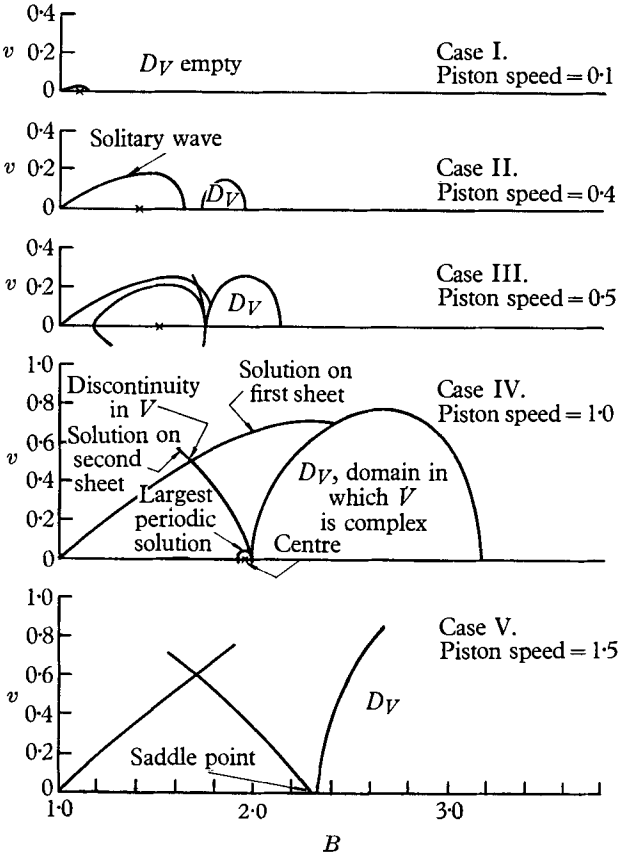

FIGURE 2. Behaviour of the steady-state solutions in the (B, v)-plane.

For the larger values of β_0 the domain D_V approaches the solitary-wave lobe from the outside. In both cases intersection occurs on the curve C_2 given by

$$2(2-\eta)^3/\eta^2(3-\eta) = \beta_0/(1+\beta_0), \tag{3.12}$$

and beyond this the solitary wave no longer exists.

This is the mathematical description of the limit to the solitary wave. Physically, the limit corresponds to the formation of an infinitely weak shock at the peak of the wave or, in the cold-plasma case, to the looping of the particle orbits. Vernon (1960) expresses the limiting condition (3.12) as

$$V_m = \nu, \quad \text{where} \quad \nu^3 = \beta_0/U^2, \tag{3.13}$$

and V_m is the value of V at the solitary-wave peak. From this form we see $|u'_m| = V_m U = (\beta_0/V_m)^{\frac{1}{2}} = (2p_m V_m)^{\frac{1}{2}}$, i.e. the fluid speed equals the characteristic speed.

As η increases beyond its value on the curve C_2 discontinuities can, and as we shall see in the numerical results, do appear in the solution. But of the main types of steady-state solution on the first sheet, i.e. that containing the initial state, only the periodic solutions exist here. Their number is gradually decreased as, with increasing η, the domain D_V approaches the second singular point (B_1, v_1). After it has reached this point, a condition represented by curve C_3 in figure 1, D_V again recedes to the right. But now (B_1, v_1) is a saddle point on the second sheet and can be joined to the initial state by the discontinuous solution. This is made up of two parts: on the first sheet there is the remnant of the solitary-wave solution issuing from the initial state with a positive dv/dB; and on the second sheet there is a solution issuing from (B_1, v_1) with a negative dv/dB. They meet at a point in the (B, v)-plane where a jump discontinuity in V, equal to the difference of the two roots of (3.4), joins them. The situation is shown as the last case in figure 2 and the form of the solution as plotted against the Lagrangian space co-ordinate is shown in figure 6.

The physical meaning of the limit on the existence of the discontinuous solution is clear from (3.9) and the ensuing discussion: in the constant states the characteristic speed $(2pV)^{\frac{1}{2}}$ equals $(\beta_i B_i)^{\frac{1}{2}}$ and the flow speed $|u'_i| = M_i B_i^{\frac{1}{2}}$; thus the condition $M_1^2 < \beta_1$ is the usual shock condition, that the flow be subsonic behind the shock, applied at the final constant state.

4. Numerical solutions of the time-dependent equations

For the numerical calculations it is most convenient to work with the equations in their Lagrangian form, taking

$$\xi = \int_0^x \rho \, dx$$

as the Lagrangian space co-ordinate. In addition, to enable the computations to be simply continued through the shock fronts we introduce a von Neumann–Richtmyer artificial viscosity q (von Neumann & Richtmyer 1950). With A/V^2 introduced for the pressure, the equations are then

$$u_t + [A/V^2 + q + \tfrac{1}{2}B^2]_\xi = 0, \tag{4.1}$$

$$V_t = u_\xi, \tag{4.2}$$

$$A_t + (qV)V_t = 0 \quad \text{where} \quad \begin{cases} qV = a^2 h^2 (u_\xi^2) & \text{if} \quad u_\xi < 0, \\ qV = 0 & \text{if} \quad u_\xi \geqslant 0, \end{cases} \tag{4.3}$$

$$B_{\xi\xi} = BV - 1, \tag{4.4}$$

where a^2 is a parameter used to control the amount of artificial viscosity introduced and h is the mesh spacing in ξ. The initial and boundary conditions are:

$$t = 0, \quad \xi \geqslant 0: \qquad B = V = 1, \quad u = q = 0, \quad A = \tfrac{1}{2}\beta_0; \tag{4.5}$$

$$t > 0, \quad \xi = 0: \qquad B_\xi = 0, \quad u = u_P(t). \tag{4.6}$$

The difference scheme used to approximate these equations is described in an appendix; it allows explicit integration of the first three equations while (4.4) is solved implicitly; all differences are centred on a staggered mesh except for the expression for q_ξ in the first equation. Criteria for the stability of the difference scheme are effectively the same as those for pure fluid dynamics, there being one for the shocked region and one for the smooth flow outside this as described, for example, by Richtmyer (1957). A running check on the computation is provided by the energy conservation integral,

$$u_P[p+q+\tfrac{1}{2}B^2]_P = \frac{d}{dt}\int_0^\infty (\tfrac{1}{2}u^2+pV+\tfrac{1}{2}B_\xi^2+\tfrac{1}{2}B^2V)\,d\xi, \tag{4.7}$$

where the suffix P is used to refer to quantities evaluated at the piston.

For illustrative purposes attention has been concentrated on five cases for each of which $\beta_0 = 0{\cdot}1$. In each case the piston is accelerated uniformly from rest to a final velocity in either one or two units of time and then held at this velocity thereafter. The five cases correspond to final velocities of 0·1, 0·4, 0·5, 1·0 and 1·5, these being chosen so as to demonstrate each of the types of solution to be

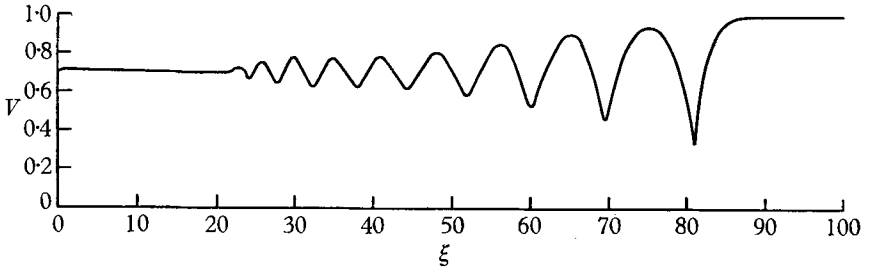

FIGURE 3. The wave-form for V at $t = 60{\cdot}0$ for case II; ξ is the Lagrangian co-ordinate.

expected from the analysis of the steady-state solutions. After an initial period in which the effect of the acceleration is dominant, the solutions settle down to a fairly common form consisting of four parts. The first, comprising the leading edge of the disturbance, starts out as an exponential then rises more steeply and possibly ends with a discontinuity: it propagates into the plasma at a speed which is eventually constant. This is followed by a wave train of increasing length, the amplitude of the waves decreasing away from the disturbance front until a constant state is reached; the constant state makes up the third portion of the solution and extends almost to the piston to which it is joined by a narrow boundary layer. Figure 3 shows a typical example.

For three of these cases a quantitative description can be given of the eventual form using only the initial and boundary data and constructing a steady-state solution from the basic solutions described in the previous section. To determine which of these basic solutions are available we need to identify each case with a point on figure 1: β_0 is given and the other parameter is matched by identifying the final piston velocity with the fluid velocity in the second constant state, thus determining η, U, etc. Using this method the five cases correspond to the points

marked with crosses in figure 1 and the situation on the (B, v)-plane for each case is shown in figure 2.

As would be expected, case V is the most straightforward: a discontinuous steady-state solution joining the initial state to the state corresponding to the piston velocity exists and our matching is therefore correct. The piston reached its final velocity at $t = 2{\cdot}0$ and by $t = 12{\cdot}5$ the front of the wave looked as in figure 6; the corresponding steady-state solution is shown on the same figure. There is very close agreement except in a region one unit wide in which the artificial viscosity resolves the discontinuity in V. The shock speed and the state behind the front agree very well too, as can be seen from table 1.

	Case I	Case II	Case III	Case IV	Case V
Piston speed ...	0·1	0·4	0·5	1·0	1·5
Steady-state solutions					
U	1·1265	1·3909	1·4888	2·0394	2·6631
(i) Constant state					
B_1	1·0974	1·4037	1·5056	1·9621	2·2897
V_1	0·9112	0·7124	0·6642	0·5096	0·4367
A_1	0·0502	0·0615	0·0710	0·1726	0·3668
(ii) Largest periodic solution					
Wavelength	∞	∞	9·80	4·45	0
A	0·0500	0·0500	0·0563	0·1719	0·3668
Time-dependent solutions	$t = 100$	$t = 150$	$t = 40$	$t = 20$	$t = 12{\cdot}5$
U	—	1·440	1·53	2·04	2·66
(i) Constant state					
u	0·1000	0·4000	0·5000	1·0000	1·5000
B	1·0998	1·419	1·530	1·970	2·291
V	0·909	0·705	0·653	0·508	0·4365
A	—	—	—	—	0·371
(ii) Wave train					
Wavelength	—	10·7	8·8	4·0	—
A	0·0500	0·0506	0·069	0·174	—

TABLE 1. Summary of the cases computed: for each $\beta_0 = 0{\cdot}1$. Limiting solitary wave occurs at $\eta = 1{\cdot}4685$, $U = 1{\cdot}4524$ at peak of which $V = 0{\cdot}3619$. Discontinuous solution exists for $\eta > 2{\cdot}1807$, $U > 2{\cdot}4198$.

In case IV the wave train behind the discontinuity appears and in case III these waves are of increased amplitude and wavelength. Parts of the solutions (at $t = 40$ and $t = 20$, respectively) are shown in figures 4 and 5: by this time the leading part of the solution has reached a steady form and the first wave of the following train is beginning to have a readily identifiable wavelength. Turning to the (B, v) diagrams in figure 2, we can see how this form is made up from the steady-state solutions. The second singularity is still on the sheet corresponding to the larger root for V and around it there is a set of periodic solutions, that with largest amplitude touching the boundary of the domain D_V at a point on the B-axis. Also passing through this point and touching D_V is a solution on the other sheet, using the smaller root for V, which eventually intersects the curve corresponding to what is left of the solitary wave. Where these two solutions and

the boundary of D_V touch is the only place where a solution may change from one sheet to the other without causing a discontinuity in V and A. Thus a solution can be made up of (i) an initial part along the solitary wave curve, (ii) a jump to the second sheet, (iii) continuation on this sheet to the point of contact with the boundary of D_V on the B-axis, ending with (iv) the continuous traversal of the

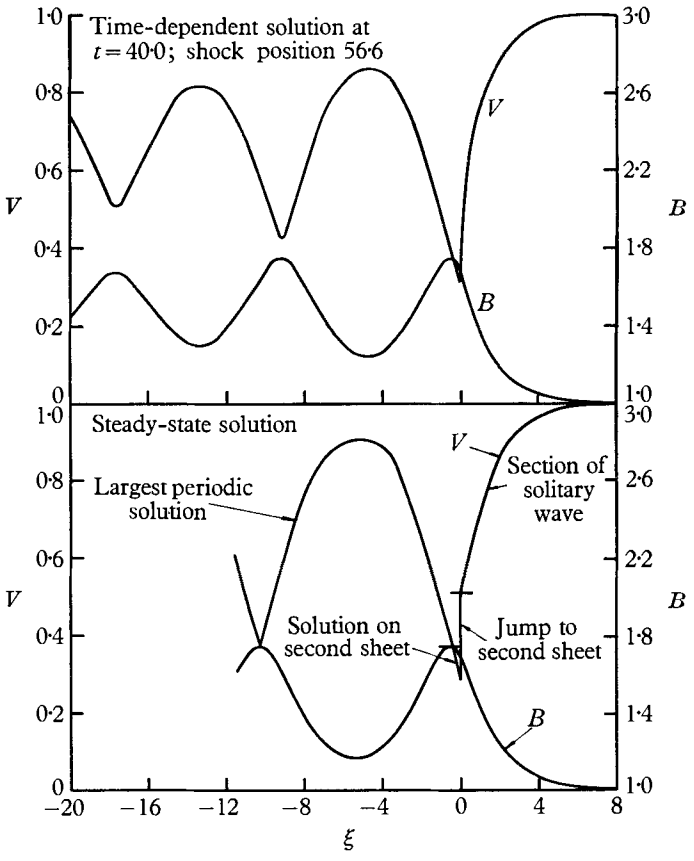

FIGURE 4. Comparison of the time-dependent solution and a composite steady-state solution for case III.

periodic-solution loop. Solutions constructed in this way are shown for cases III and IV on figures 4 and 5, below those obtained for the time-dependent problem. There is a very considerable agreement even at this early stage in the development of the wave train and with the matching of parameters described above.

In table 1 the shock velocities and the values of the variables in the constant state that develops near the piston are compared with those obtained from the steady state. As we should expect, the shock velocity and the characteristics of the wave train are consistent, their difference from the steady-state values arising mainly from incorrect choice of the parameter η; but the constant state cannot be properly compared with anything from the steady-state solutions for its entropy is that of the largest periodic solution forming the head of the wave train, and not that of the constant state at the second singularity. Further, it is

joined to the front of the disturbance by the time-dependent part of the wave train.

The values of the parameters for case II suggest that a type of solution may be obtained in which there are no discontinuities and the solitary wave plays a larger role. However, here the matching of the parameters breaks down and no description of the solution in terms of the steady-state solution has been possible

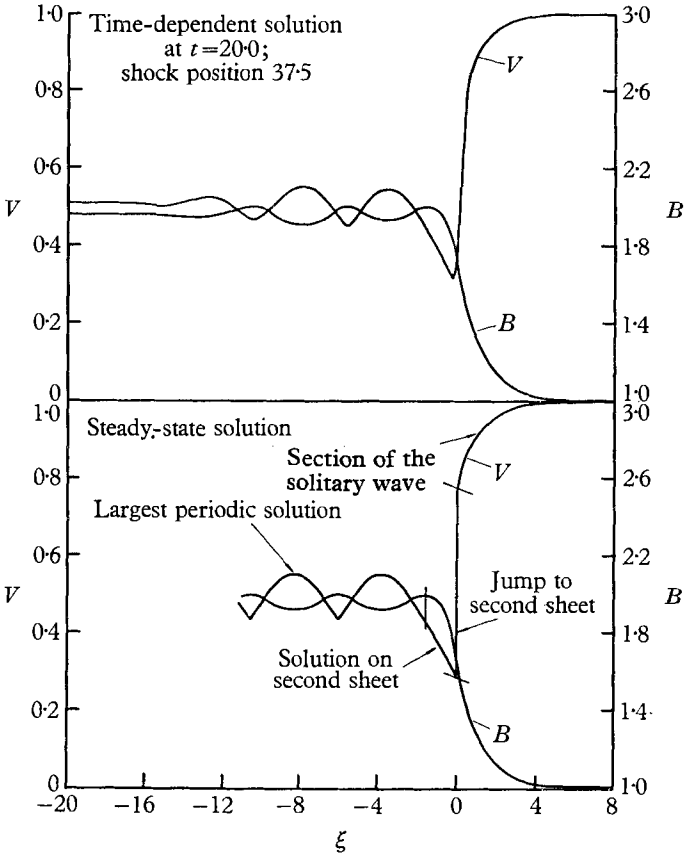

FIGURE 5. Comparison of the time-dependent solution and a composite steady-state solution for case IV.

either in this case or in case I. The speed of the wave front increases until it is larger than the critical speed of 1·4524 at which stage it breaks. This occurs at about $t = 60$ after which the speed decreases and is roughly constant between $t = 100$ and $t = 150$ when the computation was stopped. In the whole computation the most constant parameter was the wavelength of the leading waves which remained at 10·7 from $t = 100$: in contrast to cases III and IV however, the significance of this value has not been found.

The low piston speed for case I was chosen with the hope that the behaviour of the solution might approximate the asymptotic form given by Gardner & Morikawa (1960) for a cold plasma. The equations that they give can also be derived for the present case and imply that $1-B$, $1-\rho$ and $u(1+\beta_0)^{-\frac{1}{2}}$ are all

equal; moreover, in the particular solution they give, the waves have a definite amplitude related to the piston velocity and widen with time like $t^{\frac{1}{2}}$. At $t = 100$ when the integration of case I was stopped the amplitude of the waves was still growing, although it was already much greater than that predicted. None of the other features were reproduced to a useful degree of approximation.

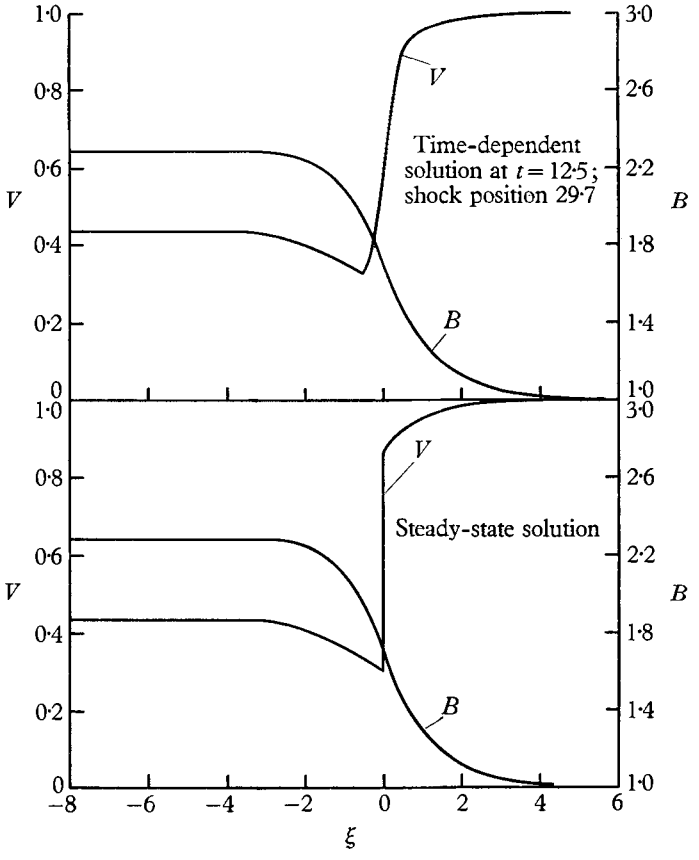

FIGURE 6. Comparison of the time-dependent and steady-state solutions for case V.

5. Discussion of the results

We have shown that when the 'shock' speed or compression is too great for the solitary wave to exist, the two-fluid equations for a warm plasma still admit steady-state solutions. These are generalized solutions involving discontinuities in the fluid variables at which entropy is gained and which lead either to periodic waves of a distinctive form or to a constant state. Moreover, in these cases the solution of the time-dependent piston problem converges to the corresponding steady-state solution in so far as this is possible: when the discontinuity is followed by a wave train the boundary condition on the piston has to be met through a time-dependent transition region.

These solutions are certainly not collisionless shocks, there being no mechanism specified for the entropy gain: they bear some resemblance to the shock within

a shock that one obtains in conventional fluid dynamics with a thermally conducting inviscid fluid. The distance scale on which the discontinuity appears is the familiar geometric mean of the ion and electron gyromagnetic radii so its resolution demands a mechanism operating on a scale length related to either the electron gyromagnetic radius or perhaps the Debye length. It may be significant that in calculating the charge separation field from the solitary-wave solution, Vernon (1960) found that it became discontinuous where the solitary wave ceased to exist: clearly the assumption of charge neutrality breaks down here.

The present work, in common with most previous studies, has been concerned exclusively with transverse waves, i.e. those in which the magnetic field is perpendicular to the direction of wave propagation at all times. Recently Saffman (1961*a*) has considered first the longitudinal case and later (1961*b*) the general case of arbitrary orientation. Working with a cold plasma, he has been restricted to relatively weak waves but has obtained waves travelling at speeds greatly in excess of the Alfvén speed and also shock-like transitions to oscillatory states behind the wave front. These occur over distances comparable with the ion gyromagnetic radius. Extensions of the numerical work described above have given similar results which will appear later.

This work was carried out while the author was on sabbatical leave from the United Kingdom Atomic Energy Authority, Harwell.

Appendix

Finite difference equations

Using a constant mesh size h and a time step k, let u be correctly centred at points $\xi = jh$, $t = (n-\frac{1}{2})k$, $(j, n = 0, 1, \ldots)$ and denote its values at these points by u_j^n; similarly let V, B and A be centred at $\xi = (j+\frac{1}{2})h$, $t = nk$, their values being denoted by V_j^n, etc.; finally qV and q will be centred at $\xi = (j+\frac{1}{2})h$, $t = (n-\frac{1}{2})k$. We then have the difference equations

$$u_{j+1}^{n+1} = u_{j+1}^n - (k/h)\{A_{j+1}^n/(V_{j+1}^n)^2 - A_j^n/(V_j^n)^2 + q_{j+1}^n - q_j^n + \tfrac{1}{2}[(B_{j+1}^n)^2 - (B_j^n)^2]\}, \tag{A. 1}$$

$$V_j^{n+1} = V_j^n + (k/h)(u_{j+1}^{n+1} - u_j^{n+1}), \tag{A. 2}$$

$$A_j^{n+1} = A_j^n - (qV)_j^{n+1}(V_j^{n+1} - V_j^n), \tag{A. 3}$$

where
$$(qV)_j^{n+1} \begin{cases} = a^2(u_{j+1}^{n+1} - u_j^{n+1})^2 & \text{if} \quad (u_{j+1}^{n+1} - u_j^{n+1}) < 0, \\ = 0 & \text{if} \quad (u_{j+1}^{n+1} - u_j^{n+1}) \geqslant 0, \end{cases}$$

$$B_{j+1}^{n+1} - (2 + h^2 V_j^{n+1}) B_j^{n+1} + B_{j-1}^{n+1} = -h^2, \tag{A. 4}$$

$$q_j^{n+1} = 2(qV)_j^{n+1}/(V_j^{n+1} + V_j^n). \tag{A. 5}$$

These equations are solved in the order given. When solving (A. 2), u_0^{n+1} is obtained from the expression for the piston velocity which is given; and (A. 4) which is implicit needs boundary conditions at each end. At the piston we have $B_{-1}^{n+1} = B_0^{n+1}$ while the other boundary is allowed to move outwards by adding points until $|B_{J+1}^{n+1} - 1{\cdot}0| \leqslant \epsilon$ where ϵ is some prescribed error. Since V decays to its value at $x = +\infty$ more rapidly than B, $|B - 1{\cdot}0|$ has a tail of the form e^{-x} and

we use this as the outer boundary condition. The tri-diagonal matrix equations for B are solved in the usual recurrence relation manner (see, for example, Richtmyer 1957).

Stability

In regions of smooth flow away from the almost discontinuous regions we may take $q = 0$. Then the amplification matrix for the variables u, V, A has the characteristic equation

$$(\lambda - 1)[\lambda^2 - (2 - 4g^2d^2)\lambda + 1] = 0, \tag{A. 6}$$

where $$g = (k/h)s, \quad s = \sin \tfrac{1}{2}mh$$

and $$d^2 = \frac{2A}{V^3} + B^2 \frac{h^2(1 - \frac{1}{3}s^2)}{4s^2 + h^2(1 - \frac{1}{2}s^2)\, V}$$

$$= 2A/V^3 + O(h^2), \quad \text{usually.}$$

Thus for all practical purposes the stability condition is the usual one, that $(h/k) > (2A/V^3)^{\frac{1}{2}}$, the sound speed in Lagrangian co-ordinates.

In the 'shocked region' the magnetic field and its first derivative are continuous so that in this narrow region the equations are identical to those of fluid dynamics: for these, Richtmyer (1957) gives the condition

$$\frac{k}{h}\left(\frac{2A}{V^3}\right)^{\frac{1}{2}} \leqslant \frac{[\eta(\eta - \frac{1}{3})]^{\frac{1}{2}}}{2a(\eta - 1)},$$

where η is the shock strength, or compression ratio of the shock.

REFERENCES

Adlam, J. H. & Allen, J. E. 1958 The structure of steady collision-free hydromagnetic waves. *Phil. Mag.* **3**, 448.

Auer, P. L., Hurwitz, Jr., H. & Kilb, R. W. 1961 Low Mach number magnetic compression waves in a collision-free plasma. *Phys. Fluids*, **4**, 1105.

Auer, P. L., Hurwitz, Jr., H. & Kilb, R. W. 1962 Large amplitude magnetic compression of a collision-free plasma. II. Development of a thermalised plasma. *Phys. Fluids*, **5**, 298.

Baños, Jr., A. & Vernon, A. R. 1960 Large amplitude waves in a collision-free plasma. I. Single pulses with isotropic pressure. *Nuovo Cimento*, **15**, 269.

Davis, L., Lüst, R. & Schlüter, A. 1958 The structure of hydromagnetic shock waves. I. Non-linear hydromagnetic waves in a cold plasma. *Z. Naturforsch.* **13***a*, 916.

Gardner, C. S., Goertzel, H., Grad, H., Morawetz, C. S., Rose, M. H. & Rubin, H. 1958 Hydromagnetic shock waves in high-temperature plasmas. *Proc. of the 2nd U.N. Intern. Conf. on the Peaceful Uses of Atomic Energy*, vol. 31, 230.

Gardner, C. S. & Morikawa, G. K. 1960 Similarity in the asymptotic behavior of collision-free hydromagnetic waves and water waves. *TID-6184, Courant Inst. Math. Sci.*, New York University.

Morawetz, C. S. 1959 Magneto-hydrodynamic shock structure using friction. *NYO-8677, Courant Inst. Math. Sci.*, New York University.

Neumann, J. von & Richtmyer, R. D. 1950 A method for the numerical calculation of hydrodynamic shocks. *J. Appl. Phys.* **21**, 232.

RICHTMYER, R. D. 1957 *Difference Methods for Initial Value Problems.* New York: Interscience.

SAFFMAN, P. G. 1961*a* Propagation of a solitary wave along a magnetic field in a cold collision-free plasma. *J. Fluid Mech.* **11**, 16.

SAFFMAN, P. G. 1961*b* On hydromagnetic waves of finite amplitude in a cold plasma. *J. Fluid Mech.* **11**, 552.

VERNON, A. R. 1960 Large amplitude waves in a collision-free plasma. *LRL-No.* 3, *Univ. of Calif.*, Los Angeles.